FLUVIAL SEDIMENTATION CONTROLLED BY DISTAL SUBAQUEOUS SEDIMENT DYNAMICS

A THESIS
SUBMITTED TO THE FACULTY OF THE GRADUATE SCHOOL
OF THE UNIVERSITY OF MINNESOTA
BY

Jeré Anthony Mohr

IN PARTIAL FULFILLMENT OF THE REQUIREMENTS
FOR THE DEGREE OF
MASTER OF SCIENCE

John B. Swenson

November 2006

ACKNOWLEDGEMENTS

I would like to thank the many people who were instrumental in allowing me to complete this milestone. First and foremost, Leah, whose love, support, and encouragement has never wavered. Also, my parents; without their loving support over the years, none of this would have been possible. The final family member I would like to thank is my dog Sasha, who always gave me a good excuse to leave the office and mangled many a plastic pop bottle in the office while I was working.

I would like to thank my advisor Dr. John Swenson and committee members Dr. Tim Demko and Dr. Vaughn Voller for their support and guidance. John's "big picture" style and endless ideas continue to be a scientific inspiration to me. Thanks to Tim for introducing me to the wonders of Utah's rocks. I would like to thank Chris Paola and the entire sedimentology group at the University of Minnesota Twin Cities, especially Ben Sheets and John Martin for assistance brainstorming and setting up experiments at St. Anthony Falls. I feel lucky for the opportunity to work with such a groundbreaking research group!

I am also grateful to the many great fellow graduate students with whom I shared my time at UMD. They provided a great sounding board for scientific ideas and a great social outlet as well (we need to go back to Fargo!!). I truly enjoyed the time I spent in the Geology department at UMD. OK – so maybe this dragged on a little longer than it needed to, but I know that I learned a great deal throughout this process and I will always carry that knowledge with me.

TABLE OF CONTENTS

LIST OF TABLES

LIST OF FIGURES

I. INTRODUCTION

Sedimentary basins are regions of prolonged subsidence of the Earth's surface (Allen & Allen, 1990). The sediments that fill these depressions, derived from surrounding erosional landscapes, provide a detailed record of tectonic and climatic forcing that the basin experienced. The ultimate goal of stratigraphy is to decipher the information contained in the basin fill to reconstruct the history of external forcing. However, finding a unique solution to this inverse problem is not trivial. Sedimentary basins do not exhibit a singular response to even relatively simple allogenic forcing. Resultant basin fill characteristics are controlled by a complex combination of physical, chemical, and biological processes that can be difficult to decouple. In addition to the signatures of allogenic forcing, stratigraphic sequences may be overprinted by signals from internal (autogenic) processes. Two techniques – quantitative modeling and sequence stratigraphy – have proven integral in the attempt to decipher the language of stratigraphy.

Stratigraphy has traditionally been a descriptive science in which quantitative techniques have been underutilized (Paola, 2000). However, starting with the simple model of Sloss (1962), quantitative analysis of stratigraphic problems has provided considerable insight, which, in concert with field data, has brought the stratigraphic community closer to being able to understand the records contained in sedimentary strata.

The concepts of sequence stratigraphy, refined at Exxon Production Research in the late 1970s (Vail et al., 1977), have revolutionized the treatment of stratigraphic problems. The introduction of these concepts initiated a wave of stratigraphic research

and stressed the importance of a comprehensive model of sedimentary basin response to allogenic forcing, especially to changes in sea level. The model was the first formal attempt by stratigraphers to understand the linkage between coeval sedimentary systems in different depositional settings. Although some aspects of the sequence stratigraphic model remain controversial, it is the closest thing stratigraphy presently has to a unifying model.

In the following sections, I discuss several concepts that are integral to the development of quantitative stratigraphy and the sequence-stratigraphic model. I then briefly outline the fundamentals of sequence stratigraphy and discuss the development of quantitative methods in stratigraphy. Following this, I tie these concepts together by introducing the specific questions addressed by this thesis.

A. BASIC CONCEPTS OF FLUVIAL SEDIMENTATION

The concept of the graded alluvial stream was initially introduced by Gilbert (1877) and expanded upon by Mackin (1948). By definition, an alluvial river at grade is in a state of dynamic equilibrium; no net aggradation or erosion occurs along a particular river reach. Lane (1955) used the concept of the graded stream to construct the following relationship, which predicts semi-quantitatively how a river reach responds to changes in water supply, sediment supply, grain size, or slope:

$$Q_s \cdot d = Q_w \cdot s \qquad (1)$$

where Q_s = sediment discharge, d = sediment grain size, Q_w = water discharge, and s = channel slope. Equation (1) represents a (dimensionally inconsistent) "balance" between sediment supply, water supply, grain size, and slope and states that a change in any of these variables will result in readjustment of the fluvial profile as shown in Figure 1.

Another concept that is critical to fluvial sedimentology and geomorphology is that of base level. Following its initial definition by Powell (1875) as the "grand" or general level to which a landscape is lowered, the term has been used in a variety of ways in the literature, often leading to confusion. As it will be used here and in the sequence-stratigraphic model discussed below, base level is the imaginary horizontal level or surface to which subaerial erosion proceeds. Effectively, then, base level is eustatic sea level (Schumm, 1993).

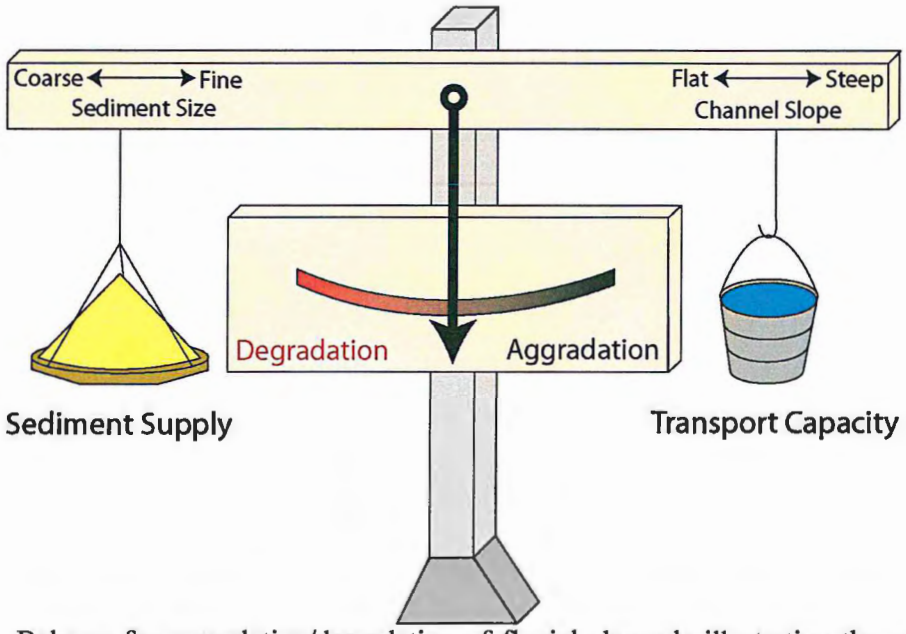

Figure 1. Balance for aggradation/degradation of fluvial channels illustrating the relationship between stream transport capacity and sediment supply. If sediment supply exceeds the transport capacity of the system, the channel will aggrade; the channel will degrade if the reverse is true. After Blum & Törnqvist (2000); based on equation (1) by Lane (1955).

B. SEQUENCE STRATIGRAPHY AND FLUVIAL SEDIMENTATION

The basic concepts of lithostratigraphy differ fundamentally from those of sequence stratigraphy. By definition, lithostratigraphy packages rocks on the basis of lithology, i.e. rock type. In sequence stratigraphy, rocks are packaged into time-significant units bounded by unconformities. The fundamental unit is a sequence, which is defined as a relatively conformable succession of genetically related strata bounded at its top and base by unconformities and their correlative conformities (Vail et al., 1977). In the sequence-stratigraphic model, bounding surfaces are time significant and, in general, cut across lithologies and facies, making them distinct from the bounding surfaces in lithostratigraphy. For reasons discussed below, the basic concepts of sequence stratigraphy are difficult to test directly in field-based studies. Hence, some ideas and details of sequence stratigraphy remain controversial (e.g. Helland-Hansen & Gjelberg, 1994), particularly the assertion by early workers that the dominant driving force in the formation of sequences is eustasy (e.g. Haq et al., 1987). Additionally, the use of confusing and sometimes contradictory terminology has been a shortcoming of sequence stratigraphy. To shift the focus of the model slightly away from purely eustatic forcing, the concepts of relative sea level and accommodation space have been used in order to account for the combination of tectonics and eustasy (Posamentier & Allen, 1999). Despite the debate over some of the details of the sequence-stratigraphic model, the formal use of time-significant surfaces to bundle packages of rocks represents a significant contribution to stratigraphy.

Sequence stratigraphy divides each sequence into "systems tracts," each of which is believed to be deposited during specific times of the relative sea level cycle. The three basic systems tracts in the Exxonian sequence stratigraphic model (there are a number of variations on the model; I focus here on the model introduced by Vail and his colleagues at Exxon Production Research) are the lowstand systems tract (LST), transgressive systems tract (TST), and highstand systems tract (HST). Each systems tract is composed of packages of parasequences, which are defined as a relatively conformable succession of genetically related beds or bedsets bounded by marine flooding surfaces or their correlative surfaces (Van Wagoner et al., 1990).

Sediments deposited during each systems tract have specific characteristics and parasequence stacking patterns that allow them to be placed in the sequence-stratigraphic framework. LST deposits consist of sediments deposited during periods of falling relative sea level, subsequent stillstand, and slow initial rise. The LST includes all deposits accumulated from the onset of relative sea level fall until sea level begins to slowly rise and shoreline transgression commences (Posametier & Allen, 1999). As the rate of relative sea level rise increases, it eventually overwhelms the sediment supply and the shoreline begins to transgress. This transition marks the onset of TST deposition. TST deposition ends when the rate of sea level rise slows sufficiently so that the sediment supply can once again drive shoreline regression. HST deposits are characterized by an increasingly progradational parasequence-stacking pattern and are interpreted to be deposited near the eustatic highstand (Posamentier & Vail, 1988). The HST ends when relative sea level begins to fall again, creating a subaerial unconformity referred to as a

sequence boundary. This sequence boundary forms the base of the subsequent LST. Of particular relevance to this study, during sequence-boundary formation, the sequence-stratigraphic model predicts that coarse-grained fluvial sediment is routed to deeper portions of the basin, where it forms a lowstand fan. Figure 2 is the oft-cited "slug diagram," which shows a schematic illustration of the sequence stratigraphic model in space and time.

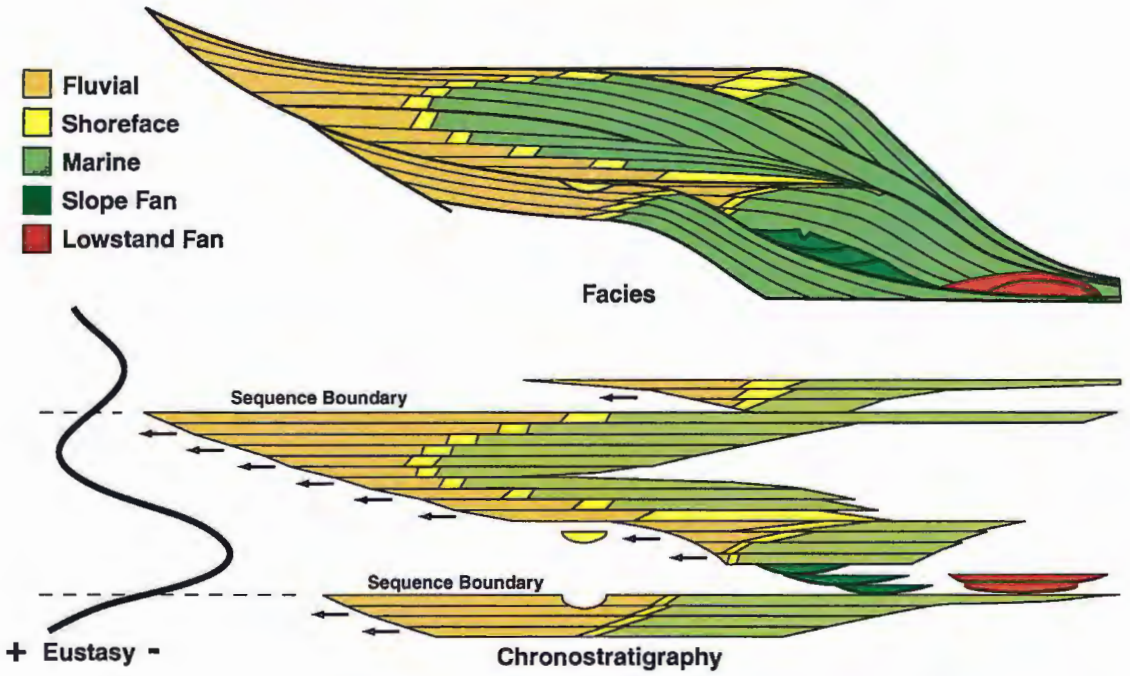

Figure 2. Slug diagram, showing facies distribution in space and time as predicted by the sequence stratigraphic model. After Haq et al. (1987).

The aforementioned concept of grade is integral to the sequence stratigraphic model and how it predicts fluvial response to changes in sea level. In sequence stratigraphy, each river possesses a fluvial equilibrium profile, which is equivalent to a graded profile as defined by Mackin (1948). Fluvial accommodation is defined as the

vertical space between the existing fluvial profile and the equilibrium fluvial profile. If the fluvial surface coincides with the equilibrium profile, the fluvial system is at grade and there is no net erosion or deposition. If the fluvial surface lies below the equilibrium profile, aggradation will result as the river strives to fill the available accommodation space. Conversely, if the fluvial surface is above the equilibrium profile, fluvial accommodation is negative and the river will incise the alluvial plain to return to a state of equilibrium (Figure 3).

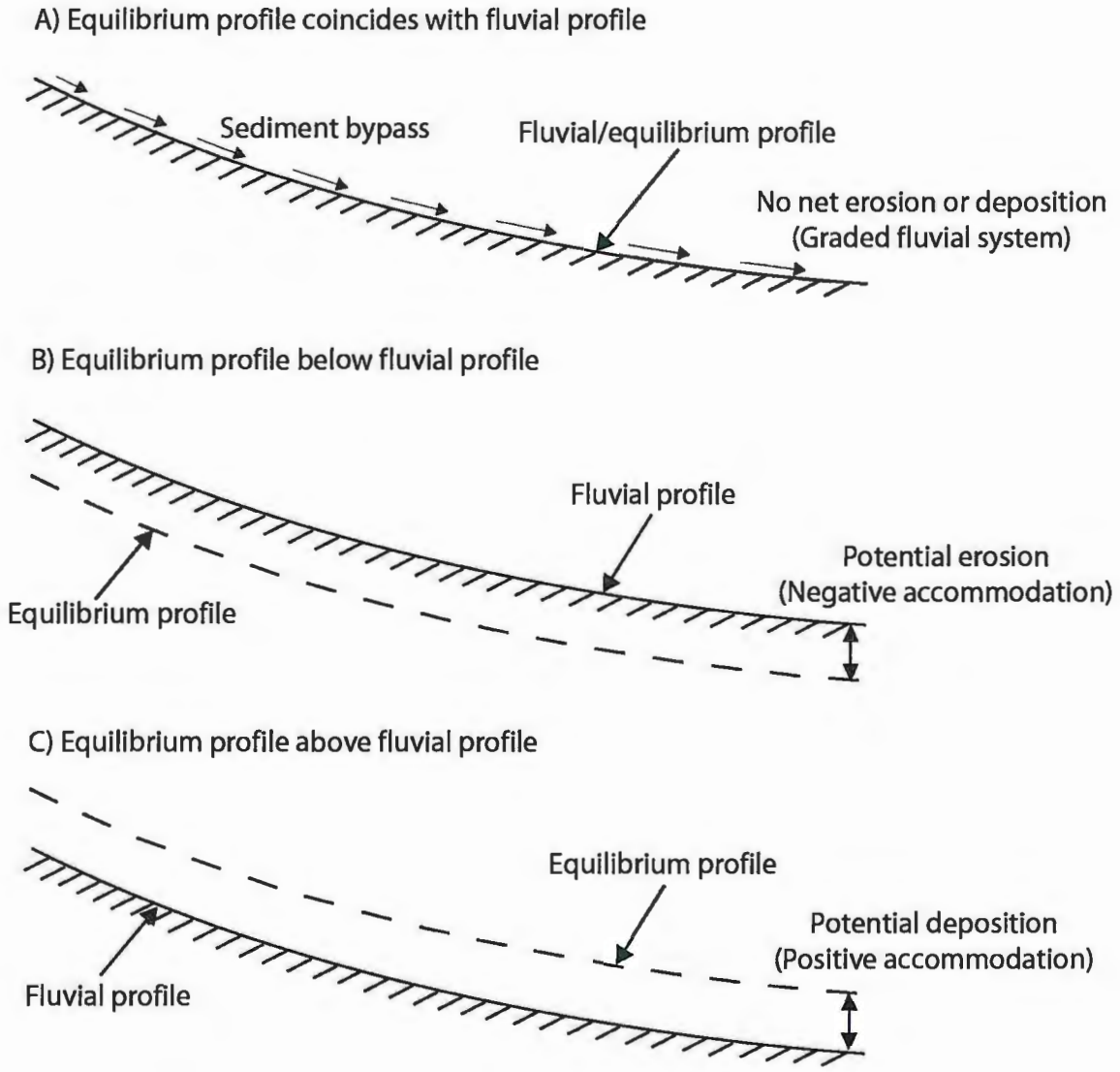

Figure 3. The concept of fluvial grade and fluvial accommodation. In (A), the fluvial profile and equilibrium profile coincide, meaning the river is graded. In (B), the equilibrium profile lies below the fluvial profile, resulting in negative accommodation and erosion. In (C), the equilibrium profile is above the fluvial profile, resulting in positive accommodation and deposition in the fluvial system. After Posamentier & Allen (1999).

The position of the fluvial equilibrium profile is strongly controlled by base level because the downstream end of the equilibrium profile is "pinned" by base level. In the sequence stratigraphic model, changes in base level (eustatic sea level) exert a strong control on

fluvial sedimentation by affecting the position of the fluvial equilibrium profile. Fluvial incision occurs during times of sea level fall (during LST), creating a sequence boundary and allowing fluvial sediment bypass to deeper portions of the basin. Field evidence of such large-scale downcutting is provided by Fisk (1944), who suggests extensive erosion of the Mississippi River valley during the last glacial lowstand. However, other studies (e.g. Saucier 1981) contradict the findings of Fisk and suggest that the effects of base level change are felt only a small distance upstream in a fluvial system. Other workers (e.g. Schumm, 1993) have suggested that rivers do not necessarily incise in response to a fall in base level. For example, a river can change its channel pattern (from meandering to braided or vice versa) or roughness in response to a change in base level; incision or erosion are not required. Fluvial system response to changes in base level remains an open question and an area of active research (Blum and Törnqvist, 2000).

In addition, upstream controls such as tectonics, sediment supply, and water supply may play a role in how fluvial systems respond to base-level change. The sequence-stratigraphic model generally assumes that upstream effects are damped well upstream of the shoreline (Posamentier and Allen, 1999, Figure 4).

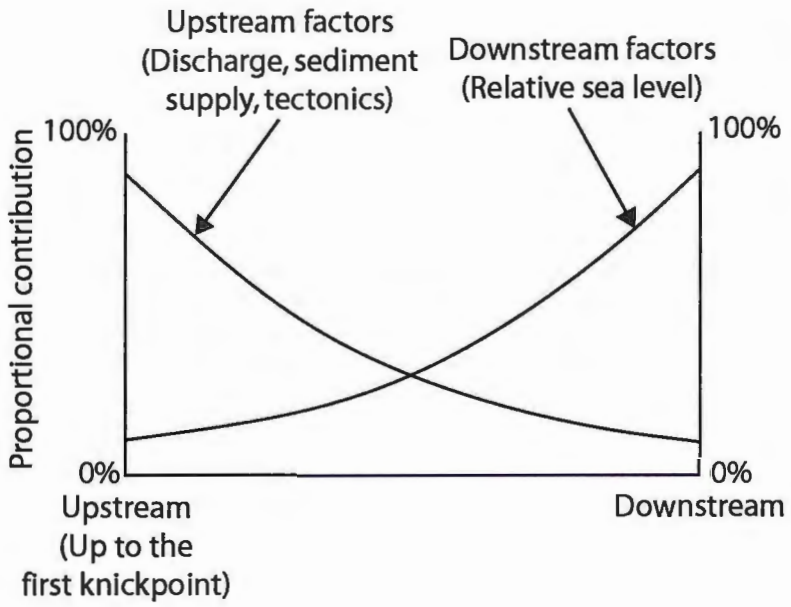

Figure 4. Relative importance of upstream and downstream controls as a function of position within the fluvial system. Toward the downstream end of the fluvial system, the effect of upstream or "local" factors becomes increasingly damped and approaches zero. Near the upstream end, the effects of changes in relative sea level become increasingly unimportant. (After Posamentier & James, 1993)

C. CLINOFORMS

The sequence-stratigraphic model is typically applied to sedimentary basins on continental margins, which are especially sensitive to changes in sea level and record these changes in their strata. The fundamental basin-filling unit for these margin systems is the clinoform, the characteristic sigmoidal geometry of prograding sedimentary bodies (Pirmez et al., 1998). As originally defined by Rich (1951), a progradational sedimentary body has three regions: the sub-horizontal, subaerial and shallow-water undaform, the steeply dipping, subaqueous clinoform, and the gently-dipping, deeper water fondoform. In current literature, the terms undaform and fondoform are not commonly used and, instead, the term clinoform is used to describe the entire progradational sedimentary

body. The parasequence is the smallest-scale clinoform in the sequence-stratigraphic model. The systems tracts and, ultimately, the sequence itself are thus formed from bundles of clinoforms.

Modern clinoforms are found on the deltas of most major river systems, including the Amazon, Ganges-Brahmaputra, Mississippi, and Yellow Rivers. Ancient clinoforms have been identified in seismic profiles and outcrop studies (Pirmez et al., 1998). The Miocene sedimentary sequences of the continental margin off New Jersey are an excellent example of clinoforms that have been very well imaged seismically (Figure 5). Outcrop examples include large-scale (amplitudes of hundreds of meters) clinoforms in the Cretaceous Western Interior Seaway deposits of the western U.S. (Swift et al., 1987) and Eocene deposits in Spitsbergen (Steel & Olsen, 2002). Smaller-scale clinoforms (amplitudes of tens of meters) have been identified in the deposits of Pleistocene Lake Bonneville of Utah (Gilbert, 1890, Milligan & Chan, 1998) and in Lake Mead (Graf, 1971, Kostic et al., 2002). The shape of clinoform surfaces is variable and is thought to be indicative of the environment of deposition and is a function of the energy in the water column and sediment grain size (Pirmez et al., 1998, Swenson et al., 2005). Sangree and Windmier (1977) defined two basic clinoform geometries – sigmoidal and oblique. Sigmoidal clinoforms have aggradational topsets and a gradual increase in slope from topset to foreset. In contrast, oblique clinoforms have topset regions with little to no aggradation and an abrupt increase in slope from topset to foreset. The foreset slope of oblique clinoforms tends to be steeper than that of sigmoidal clinoforms. This study will

generally focus on relatively small-scale oblique clinoforms, i.e. Gilbert-type deltas (Gilbert, 1890).

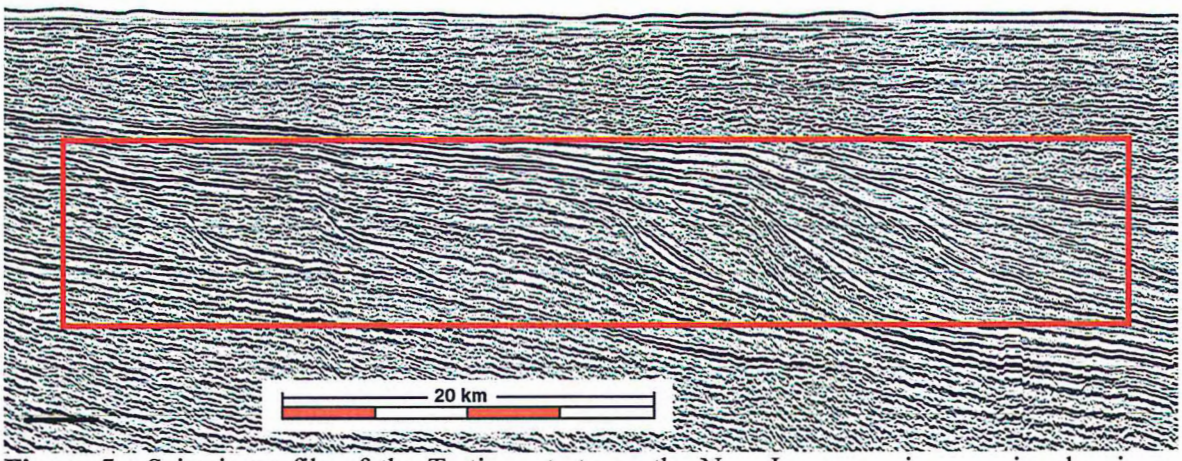

Figure 5. Seismic profile of the Tertiary strata on the New Jersey passive margin, showing clinoform geometry. Margin progradation is from left to right (from Steckler et al., 1999).

D. QUANTITATIVE STRATIGRAPHY

Historically, stratigraphy has been a predominantly descriptive science. In 1962, Sloss published a landmark paper that began to push stratigraphy in a more quantitative direction. Sloss argued that the shape of a sedimentary body is a function of four variables:

$$shape = f(Q, R, D, M) \tag{2}$$

where Q is the quantity of material supplied to the depositional site, R is the rate of subsidence, D is dispersal, a measure of the ease with which sediment moves through the system, and M represents the composition and texture of the sediment. On the basis of

these variables, Sloss predicted scenarios that would lead to large-scale transgressive and regressive cycles within a sedimentary system. Sloss' conceptual model represented an attempt to find independent, fundamental controlling variables for stratal geometry; his quantitative ideas, in combination with the concept of sea-level control espoused by Fisk (1944), would eventually became the underpinnings of the sequence-stratigraphic model. A focus of the Sloss model was the long-standing and important problem in stratigraphy of controls on regression and transgression of deltaic shorelines. Sloss (1962) and, later, Curray (1964) argued that the lateral translation of the shoreline is controlled by the ratio of sediment supply to subsidence rate. Seaward migration of the shoreline (regression) corresponds to a scenario in which sediment supply exceeds the subsidence rate, whereas transgression corresponds to the opposite scenario of subsidence rate exceeding supply. This idea is now firmly entrenched in the sequence-stratigraphic model as the '*A/S* ratio' concept.

As originally defined by Jervey (1988), accommodation (A) is defined as "the space made available for potential sediment accumulation." Sediment supply (S), is defined as the volume of sediment supplied to the basin per unit time. In the sequence stratigraphic model, the creation of transgressive, regressive, and aggradational successions depends on the interplay between A and S. The model predicts that when accommodation exceeds supply (i.e. A/S >1, a retrogradational shoreline trajectory results and overall, the system "backsteps." Conversely, a progradational shoreline trajectory results when supply exceeds accommodation (A/S < 1). In the case that accommodation and supply exactly balance each other (A/S = 1), the model predicts an

aggradational shoreline trajectory. The A/S ratio concept is directly tied to the systems tracts of the sequence stratigraphic model and is used in to predict both subaqueous and subaerial sedimentation (see discussion of fluvial accommodation and grade in the introduction). The transition from one system tract to another (i.e. from progradational to retrogradational) is the result of changes in the A/S ratio.

Muto and Steel (1997, 2000, 2002) have raised objections to the A/S ratio concept and suggested a possible redefinition. In the prevailing usage, accommodation is not treated as a three-dimensional space, but a one-dimensional quantity with the units of length, such as the water column height or the rate of relative sea level rise. Since sediment supply cannot be represented as a unit of length per time, the units of A and S do not match and therefore can never balance one another. A second problem is that, based on Jervey's definition, accommodation is inherently related to sediment supply, so the variables are not independent. Accommodation consists only of space in which sediment may be deposited, which requires the determination of the distal limit of sedimentation, an exercise that can be very difficult in practice. Finally, Muto and Steel raise objections to the use of the A/S ratio concept in subaerial settings because is relies heavily on the concept of fluvial grade, a rare condition in natural systems. This thesis will shed new light on the *A/S* ratio concept and demonstrate that it represents a specific case of a more general concept.

E. TESTING STRATIGRAPHIC THEORY

The development of quantitative models of sedimentary basins would be fruitless without a way to test them. However, poor exposure, lack of age control, and lack of knowledge of basin boundary conditions make testing stratigraphic models in the field difficult. As in other scientific disciplines, carefully controlled laboratory experiments provide a means to test theoretical models (Paola et al., 2001). Experiments allow us to generate results under precisely known, repeatable conditions (Paola, 2000). The trade off is that geologic processes occur on time and space scales that can be difficult, and sometimes impossible, to scale in a laboratory setting. It is nearly impossible to construct an exact scale model of a system involving fluid flow and sediment transport. This is chiefly due to the fact that water is the least viscous fluid available, meaning experiments will always have Reynolds numbers that are much less than those of their prototype systems. Also, it is difficult to scale sediment size to the size of the system because sediment becomes cohesive at small grain sizes. However, these problems are not unique to experiments in stratigraphy and have not prevented engineers from using scale models to solve various problems in rivers, estuaries, and coastal areas. The key point is that experiments must be conducted in conjunction with carefully thought out theoretical models. If a theoretical model can predict experimental results, it does not assure it can then be applied in the field, but if it cannot predict experimental behavior, it shows that the model must be refined before applying it to the rock record. Thus, within a theoretical framework, physical experiments provide a means to test fundamental stratigraphic principles (Paola, 2000).

F. PROBLEM STATEMENT

In this study, I address a problem that incorporates the themes discussed above. The fundamental question I attempt to answer is: How do non-eustatic processes basinward of the shoreline affect large-scale sedimentation in the fluvial system? The basic idea is that in linked depositional systems, processes seaward of the shoreline can affect the behavior of the fluvial system. To answer this question, I constructed a simple conceptual model of fluviodeltaic dynamics and then conducted a series of physical experiments at Saint Anthony Falls Laboratory, University of Minnesota, Minneapolis. The conceptual model predicts that the sediment dynamics at the base of the delta foreset exert strong control on the dynamics of the fluvial system. The results of the experiments confirm that sediment dynamics at the delta toe play an important role in fluvial sedimentation in a coupled fluviodeltaic system. This thesis presents the theoretical (conceptual) model and the results of experiments designed to test the model.

II. CONCEPTUAL & MATHEMATICAL MODEL

Below I develop a conceptual model that shows how sedimentation at the foreset toe is a critical factor in controlling fluvial sedimentation. In the second part of this section, I present a simple mathematical model that illustrates the importance of sediment dynamics at the foreset toe.

A. CONCEPTUAL MODEL

Fluviodeltaic systems prograde as approximately self-similar waveforms (clinoforms) that consist of a subaerial topset and a subaqueous foreset and bottomset (Figure 6). The net-depositional environments of the topset, foreset, and bottomset are linked at the shoreline and delta toe. It is these linkages that allow processes seaward of the shoreline to exert control on the large-scale behavior of the fluvial system. To see this, consider the idealized system of Figure 6, which is prograding across a shallow shelf under conditions of steady eustatic sea level and steady supply of sediment from an adjacent source area. (For simplicity, ignore subsidence of the shelf surface, as it does not change the central hypothesis of our conceptual model.) Let Q_{ss} and Q_{st} be the sediment discharges at the shoreline and delta toe, respectively. Standard sequence-stratigraphic models of shoreline regression and transgression directly relate the rate of shoreline migration to the sediment supply reaching the shoreline (Q_{ss}) through the 'A/S ratio' concept (Sloss, 1962; Curray, 1964; Jervey, 1988; Posamentier et al., 1988). For the system in Figure 6a, however, the rate of shoreline migration depends not on Q_{ss} alone, but on the difference in Q_{ss} and Q_{st}, which controls the fraction of overall sediment

supply deposited on the foreset. Shoreline regression and fluviodeltaic progradation requires $Q_{ss} > Q_{st}$. For a given shoreline sediment supply, an increase in Q_{st} relative to Q_{ss} decreases the amount of foreset sedimentation and, by extension, decreases the rate of shoreline advance and fluviodeltaic progradation. Because the foreset toe represents a minimum in the capacity of the linked transport system to create topography capable of maintaining the basinward flow of sediment, the dynamics of sediment transport at the toe are a critical control on foreset sedimentation and, by extension, fluvial sedimentation.

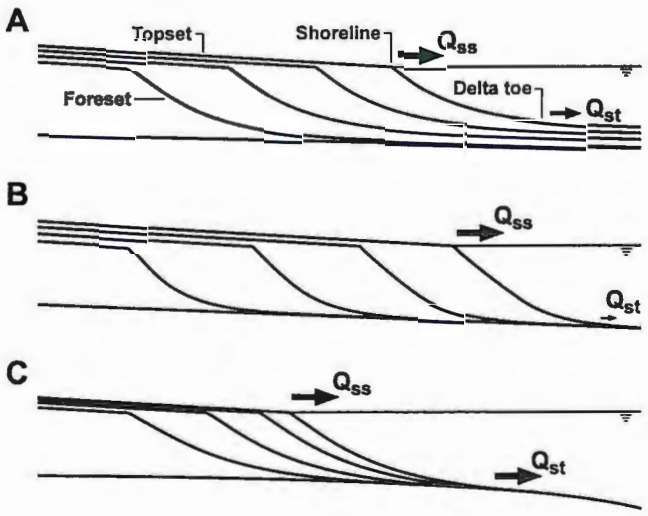

Figure 6. Conceptual model of how foreset sediment dynamics controls large-scale fluviodeltaic progradation. Difference in shoreline and delta-toe flux (Q_{ss}-Q_{st}) controls rate of foreset progradation and large-scale fluvial aggradation (A) General case. (B) Progradation and aggradation rates maximized in simple Gilbert delta, where $Q_{st} \sim 0$. (C) Decrease in progradation and aggradation rates with time as delta toe encounters progressively steeper bathymetry, thereby increasing Q_{st} relative to Q_{ss}.

But how does shoreline migration control large-scale fluvial aggradation or degradation? If the fluviodeltaic system is prograding as a roughly self-similar waveform,

then any large-scale aggradation of the fluvial surface is accompanied by shoreline regression, in order that the fluvial system maintains its transport slope. It is this connection between progradation and aggradation that provides the means for long-distance, up-dip communication between subaqueous processes on the foreset and subaerial fluvial processes. Aggradation and progradation are maximized when Q_{st} is small relative to Q_{ss}, such as might be the case with progradation of a simple Gilbert-type delta (Figure 6b). In this scenario, subaqueous avalanching maintains the foreset at a critical (failure) slope, bottomset deposition is minimal, and therefore $Q_{st} \sim 0$ (Figure 6b). Alternatively, any mechanism that increases Q_{st} relative to Q_{ss} will reduce the rate of shoreline regression and corresponding fluvial aggradation. I illustrate one such scenario in Figure 6c, which shows a delta prograding across a convex-up shelf surface. The seaward increase in shelf gradient increases the efficacy of slope-driven sediment transport on the foreset and thus increases Q_{st} relative to the fluvial sediment supply to the shoreline, Q_{ss}. As a result, the rate of foreset progradation and fluvial aggradation decreases through time. More generally, mechanisms affecting sediment "trapping" on the foreset (Q_{ss}-Q_{st}) will depend on the foreset amplitude and basin physiography and might include the frequency or magnitude of storms affecting the delta, the grain-size distribution of sediments, and the mode of sediment dispersal on the foreset, e.g. avalanching, creep, hyperpycnal flows, rainout from hypopycnal flows, etc.

B. MATHEMATICAL MODEL

Consider a progradational fluviodeltaic system such as that illustrated in Figure 7. Ignoring subsidence and sediment compaction, global conservation of sediment volume gives the growth rate of the fluviodeltaic system:

$$Q_{so} - Q_{st} = \frac{d}{dt}\int_0^u (\eta - b)dx \tag{3}$$

where Q_{so} is the sediment supply to the system and Q_{st} is the sediment flux at the foreset toe. Expanding the right-hand side of (3) gives:

$$Q_{ss} - Q_{st} = [\eta(s) - b(s)]\frac{ds}{dt} + \frac{dA_\Delta}{dt} \tag{4}$$

where Q_{ss} is the sediment flux delivered to the shoreline by the fluvial system, $\eta(s) - b(s)$ is the thickness of the fluviodeltaic system at the shoreline, and A_Δ is the cross-sectional area of the subaqueous delta. Equation (4), which is a generalized form of the shoreline-Stefan condition in Swenson et al. (2000), partitions the flux discontinuity, Q_{ss}-Q_{st}, between shoreline and foreset toe (left-hand side) into shoreline translation and temporal changes in the cross-sectional area of the subaqueous delta (right-hand side).

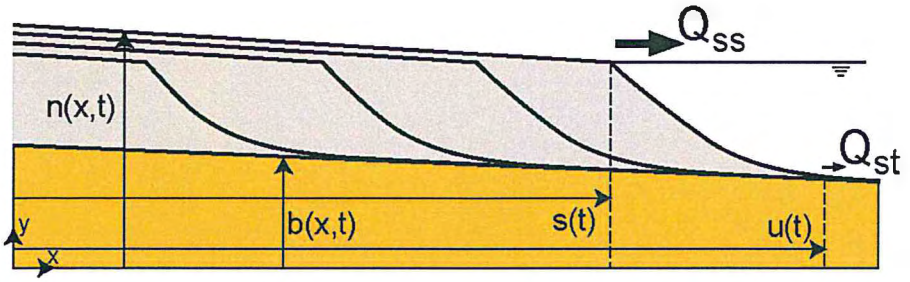

Figure 7. Definition sketch for fluviodeltaic system used in mathematical model.

Consider the limiting case of a fluviodeltaic system prograding across a flat-bottomed basin as a self-similar waveform, in which case (4) reduces to:

$$Q_{ss} - Q_{st} = H\frac{ds}{dt} \tag{5}$$

where H is the (constant) water depth in the basin and, by extension, the thickness of the sediment package at the shoreline.

According to (3), the sediment flux Q_{ss} and the sedimentation rate (divergence in flux) at the foreset toe are key controls on the rate of shoreline migration; hence, the foreset toe represents a critical point in the linked depositional system. The crucial role of the toe arises because it represents a minimum in the capacity of the transport system to create topography capable of maintaining the flow of sediment. If the sediment flux at the toe vanishes, i.e. if all sediment reaching the shoreline is trapped on the foreset, then $Q_{ss} = 0$ and the sedimentation rate at the foreset toe and rate of shoreline advance are maximized. With the rate of shoreline regression maximized, it follows that the rate of

fluvial aggradation is likewise maximized. Conversely, if sediment dynamics at the toe prevent deposition on the foreset, i.e. if the sediment fluxes at the shoreline and toe are equal so that sediments completely bypass the foreset, then the rate of shoreline advance is zero. In this scenario, the fluvial system can, in principle, attain grade (Mackin, 1948) and bypass all sediment to the deep-marine environment (Figure 8).

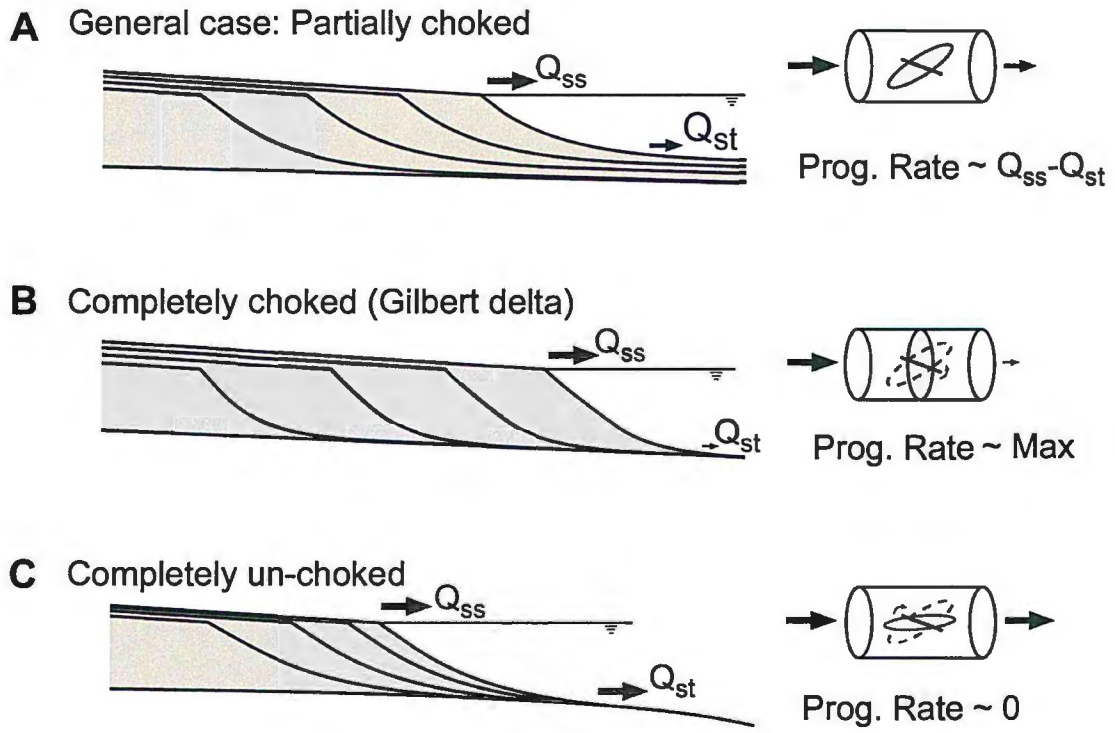

Figure 8. Three scenarios for clinoform progradation, emphasizing the importance of sediment dynamics at the clinoform toe as a control on fluvial sedimentation. (A) General case, where some sediment reaching the shoreline is deposited on the foreset and some sediment bypasses the foreset and is deposited deeper in the basin. (B) Clinoform system where all sediment reaching the shoreline is deposited on the foreset. In this case, the rate of shoreline regression is maximized, and, by extension, the rate of fluvial aggradation is maximized. (C) Clinoform system in which all sediment reaching the shoreline bypasses the foreset. In this case, shoreline regression halts as does deposition in the coupled fluvial system. In this scenario, the fluvial system can attain grade.

C. DISTAL CONTROLS ON FLUVIAL SEDIMENTATION

We focus here on the role of incipient basin physiography and hyperpycnal flows in increasing Q_{st} relative to Q_{ss} and thus decreasing the rate of large-scale fluvial aggradation.

PRE-EXISTING BASIN TOPOGRAPHY

Consider again the fluviodeltaic system of Figure 6C, which is prograding across a shelf surface with a seaward-increasing topographic gradient. If the delta toe of the prograding system encounters a bathymetric slope greater than the critical transport slope of the foreset, then sediment can no longer accumulate at the toe ($Q_{st} \sim Q_{ss}$), thereby arresting foreset progradation and fluvial aggradation. This simple scenario might be realized near the shelf-slope transition of continental margins or near the rollover (topset-foreset transition) on drowned (relict) clinoform surfaces. Geologically, this scenario may represent clinoforms that have prograded to near the shelf edge and are beginning to interact with steeper slopes. Such systems have been referred to as "shelf-margin deltas" by Porębski and Steel (2003). Presently, the delta being constructed by the Sepik River in northern Papua New Guinea is close to the shelf edge. Due to active tectonics in the region, the slope basinward of the shelf is very steep and the majority of sediment reaching the shoreline is routed offshore via a submarine canyon that extends nearly to the river mouth (Walsh & Nittrouer, 2003).

HYPERPYCNAL FLOWS

Alternatively, consider a scenario in which a change in tectonic or climatic conditions increases the input fine-grained sediment to the fluvial system. Such an increase in wash load may increase the density of fluvial outflow and result in density-driven flows across the delta foreset. Kostic et al. (2002) showed that turbidity currents passing over the delta foreset could reduce the foreset slope significantly. If the foreset slope is reduced so that it is less than the basement slope, sediment will not accumulate at the base of the foreset and the fluvial sediment flux delivered to the shoreline will bypass the foreset entirely. The change in sedimentation dynamics at the toe will then propagate upstream, ultimately affecting the entire fluviodeltaic system (Figure 8C). With the foreset toe "frozen," shoreline regression will halt. Additionally, the fluvial portion of the system will change from a depositional regime to a bypassing surface. Coarse-grained sediment will be routed to the deep marine portion of the system and deposited on deeper portions of the continental slope.

III. EXPERIMENTAL METHODS

To investigate how processes at the delta toe control sedimentation in the fluvial system, I conducted a series of flume experiments designed to test the conceptual model discussed in the previous section. In this section, I describe the experimental techniques and procedures.

A. FLUME CONFIGURATION

I conducted the experiments in a narrow, glass-walled flume 15 cm wide by 12 m long. I used only the upstream 4 m of the flume for the active portion of the experiments. At the downstream end of the flume, an adjustable gate acted as a weir, allowing a constant water level (base level). Overflow from the weir exited the flume and discharged into a nearby drain. At the upstream end of the flume, water was supplied with a fixed head tank to maintain a steady flow rate. The tank consisted of a small tank nested inside of a larger tank. Water was supplied to the inner tank with a hose at a flow rate greater than the flow rate to the flume so that the inner tank overflowed and thus water level was held constant. The overflow was captured by the outer tank, which was attached to another hose that routed the overflow water to the drain. The discharge to the flume could be controlled by an adjustable valve at the bottom of the inner tank.

Inside the flume, I placed a ramp with a horizontal portion and a sloping portion to represent the shelf-slope bathymetry of continental margins. In each experiment, I built a fluviodeltaic clinoform in the flume with a steady supply of water and fine silica sand (120 μm median diameter). I fed the sand using a small screw feeder with an

adjustable feed rate. Base level was held fixed during each experiment. During the initial phase of each experiment, a delta prograded into the basin and a fluvial system developed. When the clinoform toe reached the sloping portion of basement, I attempted to "un-choke" the system with one of the mechanisms discussed above.

B. BASEMENT GEOMETRY EXPERIMENTS

In the first set of experiments, I investigated the effect of pre-existing topography on the dynamics of the clinoform system. The submerged angle of repose for 120 μm sand is approximately 31.5°. I ran two experiments, one with the angle of the sloping portion of the ramp much less than the angle of repose (15°) and one with the sloped portion set at an angle much greater than the angle of repose (50°). Flume configurations for the basement geometry experiments are shown in Figure 9. During each experiment, I recorded the shoreline position and elevation at four points along the fluvial surface every five minutes. In addition, we documented each experiment with high-resolution digital video. The water and sand feed rates for the basement geometry experiments were approximately 28 mL/s and 2.3 g/s, repsectively.

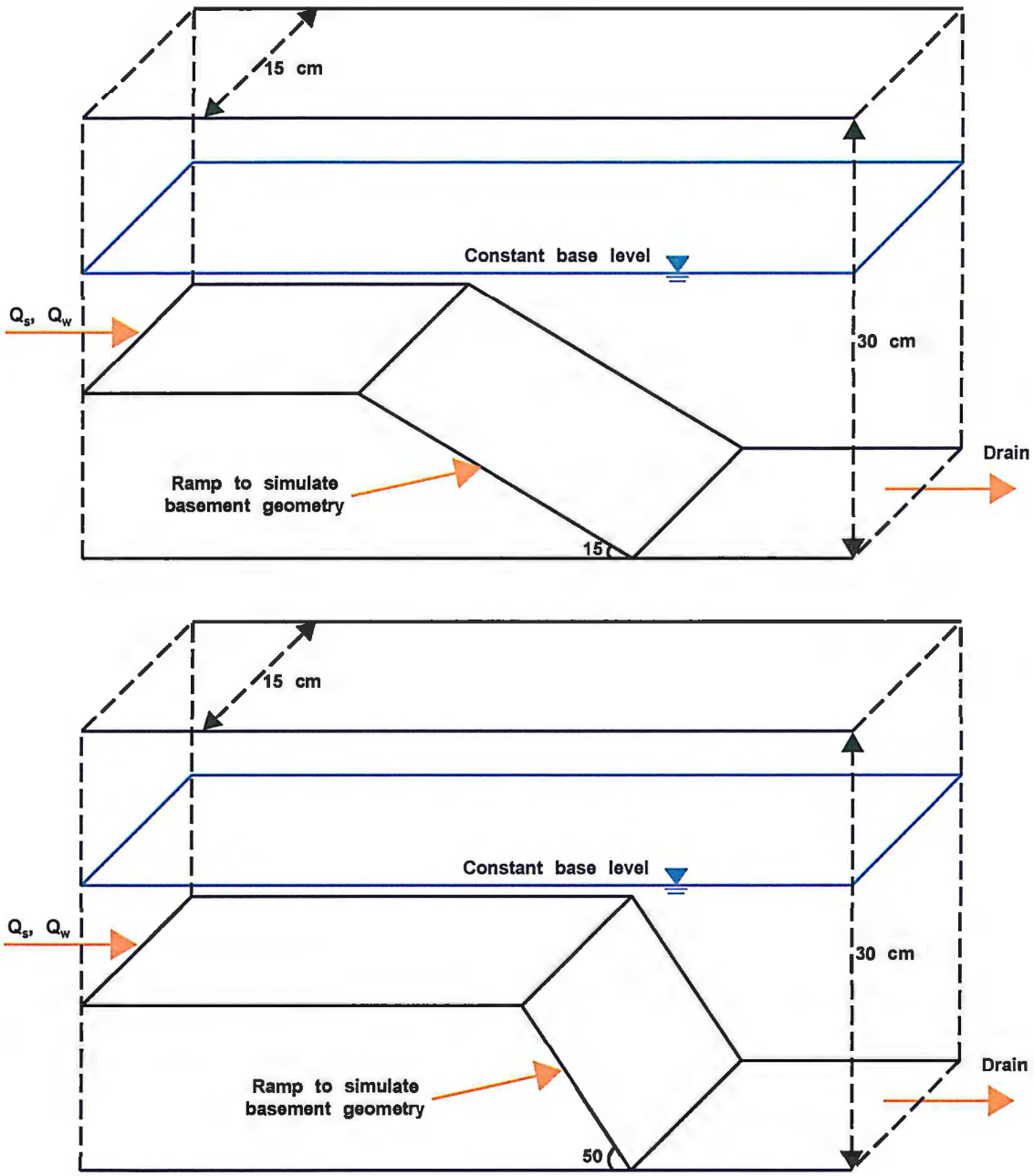

Figure 9. Flume configurations for basement geometry experiments.

C. TURBIDITY CURRENT EXPERIMENTS

In the second set of experiments ("turbidity current experiments"), I introduced silica silt (24 μm median diameter) into the sand and water feed after the clinoform toe had reached the sloping portion of the ramp. The majority traversed the fluvial system as washload, while a small fraction was deposited in the fluvial portion of the system. The small amount of silt deposited in the fluvial system did not alter fluvial aggradation rates significantly. A small fraction (~7% by weight) of the silt was composed of grains in the sand range (> 62.5μm), which likely accounts for the silt deposited in the fluvial system. The entrained silt effectively increased the density of the sand/water mixture and caused the initiation of turbidity currents at the shoreline. I ran twelve experiments with silt concentrations ranging from approximately 2% to 6% by volume. The ramp slope for these experiments was set to 25.8°, which is approximately 20% less than the submerged angle of repose for the sand (Figure 10).

I documented each experiment with a series of high-resolution digital images captured at 15 second intervals. I processed each image to construct profiles of the clinoform surface, which allowed me to track the fluvial surface elevation, shoreline position, and location of the clinoform toe as a function of time during each experiment. I discuss the image processing procedure in the following section. Table 1 provides a summary of the sediment and water feed rates for each of the experiments.

Experiment	Water Discharge (mL/s)	Sand Feed Rate (g/s)	Silt Feed Rate (g/s)
No turbidity currents	15.07	0.48	--
2% turbidity currents	15.07	0.48	0.95
4% turbidity currents	15.07	0.48	1.84
6% turbidity currents	15.07	0.48	2.78

Table 1. Water and sediment feed rates for the turbidity current experiments.

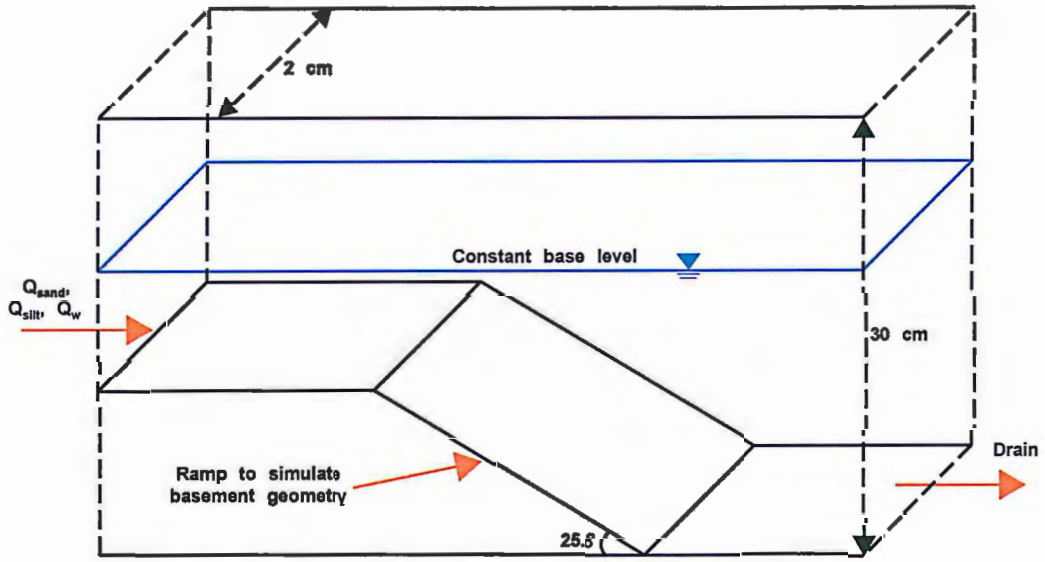

Figure 10. Flume configuration for turbidity current experiments. The ramp angle was set at 25.8 °, approximately 20% less than the angle of repose for the sand used.

D. IMAGE PROCESSING

I processed the images obtained during the turbidity current experiments in order to reconstruct the clinoform profile at each time step during the experiment. Initially, I processed them using the LensDoc filter for Adobe Photoshop, which allows for three corrections to be made to each image. The first correction made is for lens barreling, a lens distortion that causes straight lines to bow outward. The second correction was for

pincushioning, a lens distortion that causes straight lines to curve inward. Finally, each image was rotated so that known horizontal lines in the image were truly horizontal. The filter makes three adjustments simultaneously, helping to preserve image quality. I obtained the proper adjustments for each image by performing the corrections to a calibration photograph taken prior to the experiments. Since the camera remained stationary during the experiments, I was able to apply the same corrections to each image in order to obtain true profile images of the clinoform every 15 seconds. Following correction with LensDoc, I cropped each image.

To obtain clinoform profile data (i.e. $\eta(x)$ for each image), I processed each corrected image with a custom application that found the clinoform surface in the image. The program traversed each column of pixels in the image and found the top of the clinoform based on color criteria. The position of the first occurrence of a pixel meeting the specified criteria was exported to a Microsoft Excel worksheet to facilitate data analysis. Each image contained 3,008 columns of pixels, thus 3,008 data points were obtained for each image. Each experiment consists of 280-300 images, so a data set for an individual experiment contains 842,240-902,400 data points. Following collection of the clinoform surface profile of each image, I processed the data to account for erosion and reconstruct stratigraphic profiles of each experiment.

IV. RESULTS

A. BASEMENT GEOMETRY EXPERIMENTS

Shoreline position and fluvial surface elevations as function of time for the basement geometry experiments are shown in Figure 11. For the understeepened case (ramp slope = 15°), shoreline regression and fluvial aggradation continued after the toe encountered the sloping portion of the ramp because deposition of sediment at the clinoform toe was not inhibited by the change in basement geometry. Despite being fully choked, i.e. $q_s(u) = 0$, the shoreline regression rate decreased gradually after encountering the slope break due to the increase in space for the sediment to fill. In the context of Equation (2), $dA_\Delta/dt \neq 0$, which effectively reduces ds/dt. In the oversteepened case (ramp slope = 50°), shoreline regression and fluvial aggradation ceased when the clinoform toe reached the sloping portion of the ramp (~ 65 minutes), because sediment could no longer accumulate at the clinoform toe. The periodic changes in shoreline regression rate throughout the experiments, especially the 15° case, were due to channelization of the fluvial system. I measured the shoreline position on the glass walls of the flume. As the fluvial channels migrated across the fluvial surface, sediment supply to the shoreline near the walls of the flume was temporarily reduced, slowing the shoreline regression rate. As a channel shifted back to a position near the flume wall, the shoreline in that part of the flume was able to prograde. While the experimental complications due to fluvial channelization did not prevent the experimental verification of my hypothesis, I reduced the width of the flume for the turbidity current experiments to inhibit channelization and facilitate data

collection. The reduction in flume width also has the advantage of significantly reducing experimental run times.

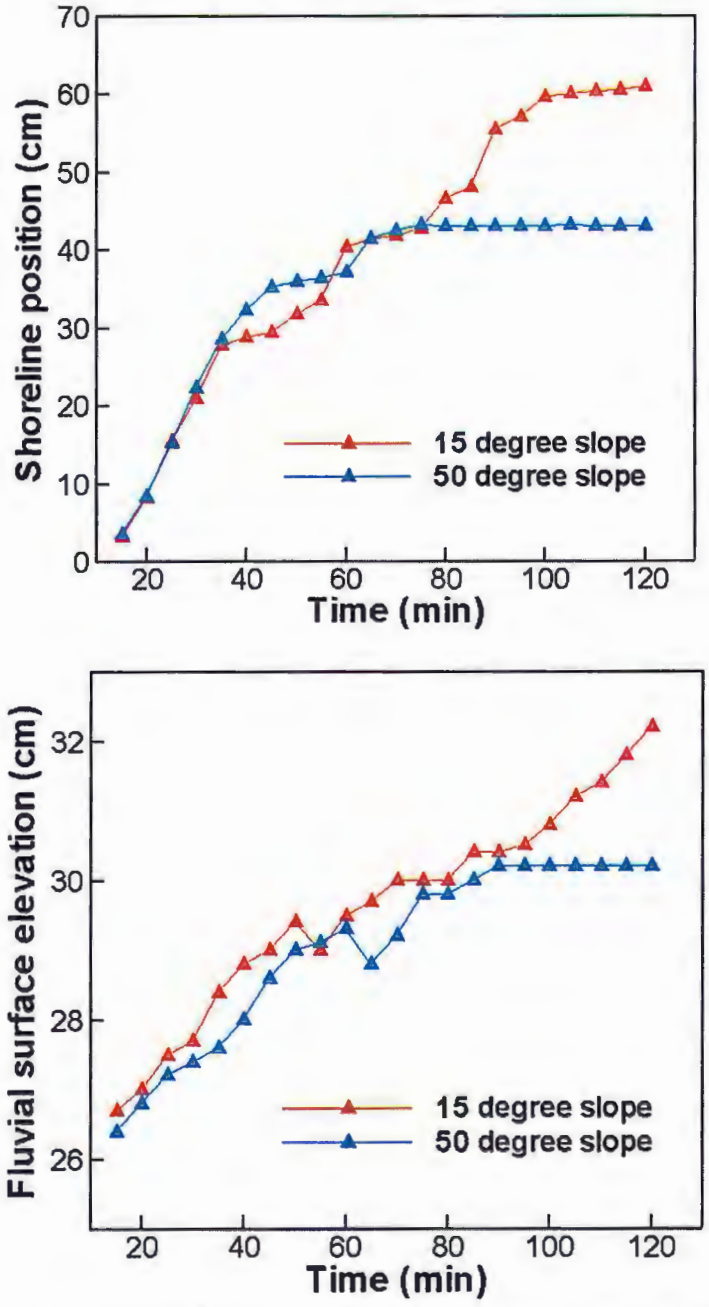

Figure 11. Shoreline position and fluvial surface elevation as a function of time for basement geometry experiments.

B. TURBIDITY CURRENT EXPERIMENTS

The impact on the experiment of introducing turbidity currents varied depending on their bulk volumetric sediment concentration. Low concentration turbidity currents (2%) did not reduce the foreset slope below the ramp angle and so did not inhibit clinoform progradation and shoreline regression. The introduction of higher concentration (> 4% silt by volume) turbidity currents, however, caused a significant decrease in the foreset slope (average 25%) such that it was lower than the ramp angle (Figure 12).

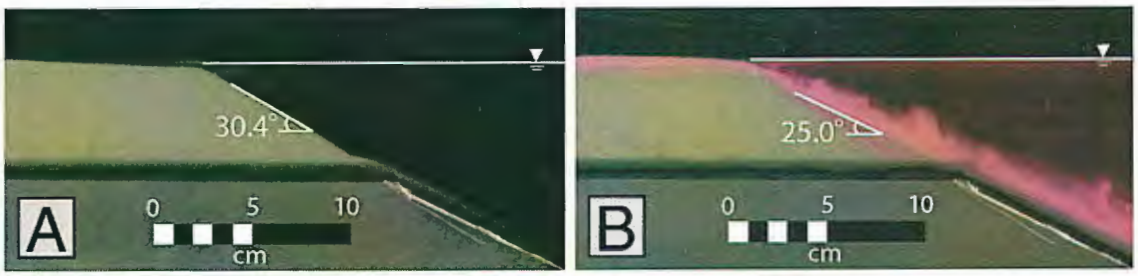

Figure 12. Comparison of foreset angle for clinoform with no turbidity currents and clinoform with turbidity currents passing over the foreset. (A) Clinoform prograding at the angle of repose with no turbidity current influence. (B) Foreset slope has been reduced (~18%) due to increased shear stress from overpassing turbidity current.

As a result, in the higher concentration experiments, sediment was unable to accumulate at the clinoform toe, thereby "un-choking" the system and allowing sand to bypass the foreset and accumulate at the base of the ramp in a subaqueous fan (Figure 13). Sediment bypassing halted shoreline regression and in fact triggered a shoreline transgression due to the reduction of the foreset slope. The slope reduction initiated knickpoints ~2 cm in magnitude that nucleated at the shoreline and propagated upstream, incising the fluvial system (oscillations in Figure 14B). Even after the foreset slope was lowered to a stable bypassing angle, slight oscillations about that angle due to the interplay between deposition and erosion on the foreset continued to generate

knickpoints. These knickpoints formed every few minutes and, at times, several knickpoints were present in the fluvial system.

Knickpoint generation was an autocyclic response of the system to the first large reduction of the clinoform foreset slope, which occurred when turbidity currents were initiated, and to subsequent, smaller-scale reductions as the foreset oscillated about a bypassing angle, which is the reduced subaqueous angle of repose in the presence of overriding turbidity currents (Kostic et al., 2002). During each phase of clinoform progradation that preceded a slope reduction, the fluvial system aggraded and prograded. Foreset oversteepening and subsequent reduction drove a shoreline transgression and the fluvial system was forced to incise via upstream migrating knickpoints to maintain an equilibrium profile.

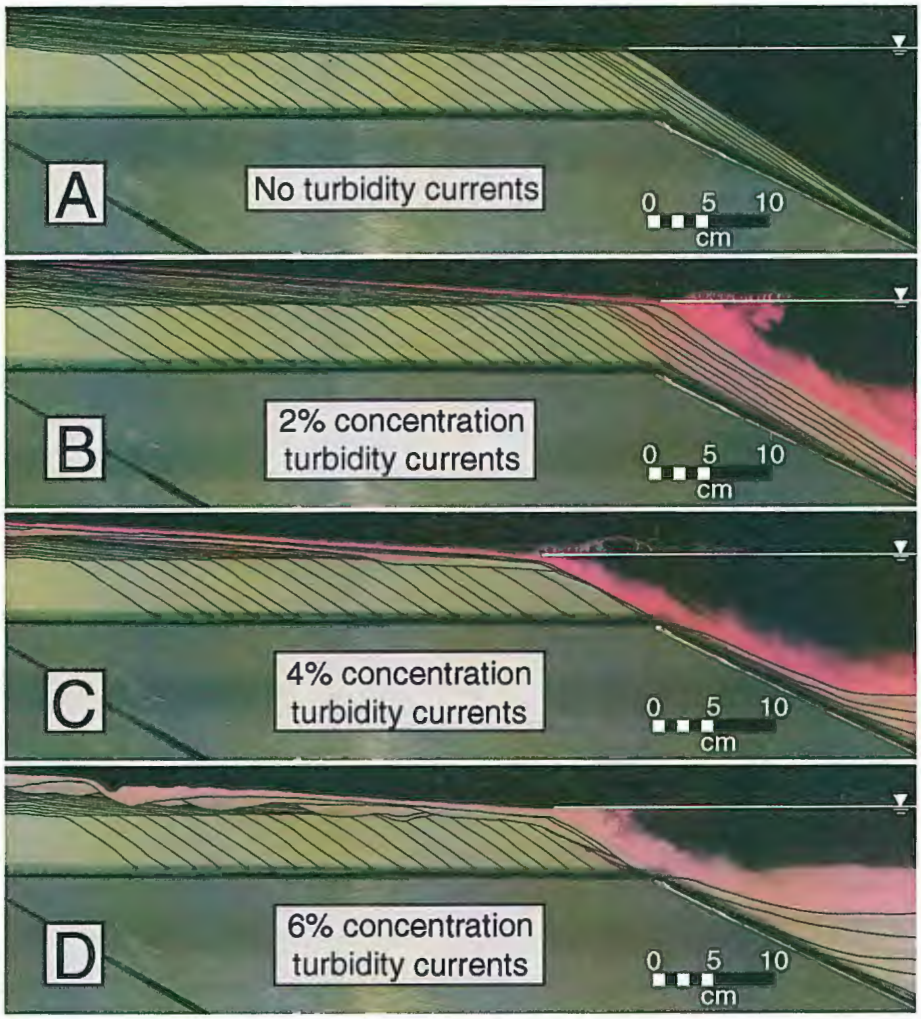

Figure 13. Reconstructed stratigraphy for turbidity current experiments. Interval between lines is 2 minutes. (A) Resultant stratigraphy of an experimental run with no turbidity currents. Note undisturbed fluvial strata and uninhibited foreset progradation onto the sloping ramp. (B) Resultant stratigraphy of an experimental run with turbidity currents of concentration ~ 2%. Foreset slope was not reduced sufficiently to arrest progradation and fluvial aggradation. (C) Stratigraphy for a run with turbidity currents ~ 4% concentration. Note cut and fill of fluvial system due to knick-point propagation and subsequent deposition. Also note deposition of material at the base of the slope, forming a subaqueous fan. (D) Stratigraphy for a run with turbidity currents of ~ 6% concentration. Fluvial system has been more extensively reworked than in the 4% experiments.

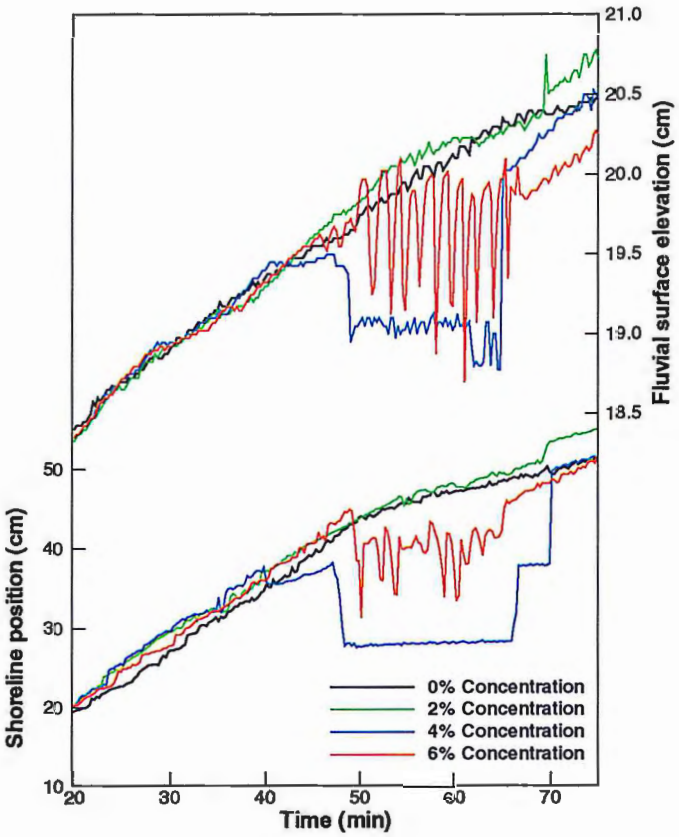

Figure 14. Shoreline trajectories and fluvial surface elevations as a function of time for turbidity current experiments.

C. Scaling Turbidity Current Experiments

I performed the turbidity current experiments with sediment sizes commonly found in nature (sand and silt), but with flow rates several orders of magnitude lower than those found in natural systems. As such, the ~ 20% reduction in foreset slope observed in my experiments is modest compared to what would be observed in a full-scale system. To address this issue, I performed densimetric Froude number scaling following the methodology of Kostic et al. (2002).

A turbidity current passing over the sand grains on the delta foreset exerts both drag and lift forces on the exposed grains. The following equation allows for calculation of the equilibrium foreset slope angle of the delta foreset in the presence of a turbidity current (see Kostic et al., 2002 for detailed derivation):

$$\tan\theta_a = \tan\theta_{ao}\left(1 - \frac{1}{\cos\theta_a}\frac{\tau_t^*}{\tau_{co}^*}\right) \tag{6}$$

where θ_a is the critical angle for the onset of grain avalanching in the presence of a turbidity current, θ_{ao} is the angle of repose of the sediment when there are no turbidity currents (typically 30-40° for sand), τ_t^* is the critical Shields stress in the presence of a turbidity current, and τ_{co}^* is the critical Shields stress for the onset of motion on a horizontal bed (typically taken as 0.03 – 0.04 (Graf, 1971)). Equation (6) can be solved iteratively for θ_a. Solutions for various values of τ_{co}^* are presented in Appendix A.

As a check of Equation (6), I examine the limiting case of a delta with no overriding turbidity current. In this case, $\tau_t^* = 0$, implying that $\tan\theta_a = \tan\theta_{ao}$, or equivalently $\theta_a = \theta_{ao}$. Physically, this means that if there are no turbidity currents, a Gilbert delta with foreset angle equal to the angle of repose is produced. As τ_t^* increases (the turbidity current becomes stronger) and approaches τ_{co}^*, θ_a decreases and approaches zero. In the limiting case of a turbidity current with $\tau_t^* = \tau_{co}^*$, $\theta_a = 0$. In reality, the slope reduction process is self-limiting because a lower foreset angle pushes the turbidity current plunge point basinward. As a result, less of the foreset is directly affected by the

overriding current, limiting the amount of slope reduction that can occur (Kostic et al., 2002).

A densimetic Froude number for the flow is defined as

$$Fr_d = \frac{U}{\sqrt{RgCH}} \tag{7}$$

where U is a flow velocity scale, R is the submerged specific gravity of the fine-grained material, g is the acceleration due to gravity, C is the volumetric concentration of fine-grained material, and H is an upward normal length scale.

For Froude number similarity, we require the following condition to be satisfied:

$$(Fr_d)_p = (Fr_d)_m \tag{8}$$

The subscript "p" denotes prototype (full-scale system) and the subscript "m" denotes the model (flume experiment).

Under the assumption that R is the same in both model and prototype, combining equations (7) and (8) gives

$$\frac{(U)_p}{(U)_m} = (\lambda_H \lambda_C)^{1/2} \tag{9}$$

where

$$\lambda_H = \frac{(H)_p}{(H)_m} \tag{10a}$$

$$\lambda_C = \frac{(C)_p}{(C)_m} \tag{10b}$$

The boundary shear stress τ_b due to the overpassing turbidity current can be estimated by

$$\tau_b = \rho C_f u^2 \tag{11}$$

where ρ is density, C_f is a friction coefficient, and u is a layer averaged velocity of the turbidity current. We assume a Manning-Strickler resistance relation where C_f varies with flow depth to the negative 1/6 power. Therefore,

$$\frac{(C_f)_p}{(C_f)_m} = (\lambda_H)^{-1/6} \tag{12}$$

The sediment sizes in the prototype and model are $(D)_p$ and $(D)_m$, respectively and

$$\frac{(D)_p}{(D)_m} = \lambda_D \tag{13}$$

The critical Shields stress in the presence of a turbidity current is given by

$$\tau_t^* = \frac{\tau_{tb}}{\rho R g D} \tag{14}$$

Combining this with the Equation (11) gives the following equations for the model and prototype:

$$(\tau_t^*)_m = \frac{(\tau_{tb})_m}{\rho_m R_m g D_m} = \frac{(C_f)_m U_m^2}{R_m g D_m} \tag{15a}$$

$$(\tau_t^*)_p = \frac{(\tau_{tb})_p}{\rho_p R_p g D_p} = \frac{(C_f)_p U_p^2}{R_p g D_p} \tag{15b}$$

Combining these two equations along with the assumption that $R_m = R_p$ gives

$$\frac{(\tau_t^*)_p}{(\tau_t^*)_m} = \left(\frac{(C_f)_p}{(C_f)_m}\right)\left(\frac{D_m}{D_p}\right)\left(\frac{U_p}{U_m}\right)^2 = (\lambda_H)^{-1/6}(\lambda_D)^{-1}((\lambda_H \lambda_C)^{1/2})^2 \tag{16}$$

Simplifying, we obtain

$$\frac{(\tau_t^*)_p}{(\tau_t^*)_m} = (\lambda_H)^{5/6}(\lambda_C)(\lambda_D)^{-1} \tag{17}$$

Using this equation, we can scale our flume experiments up to field scale. We determine $(\tau_t^*)_m$ by plugging experimental data into Equation (6). By selecting appropriate values

for λ_H, λ_C, and λ_D, we can calculate $(\tau_t^*)_p$ using Equation (17). Then, going back to Equation (6), we can calculate θ_a, the equilibrium foreset angle under the influence of an overpassing turbidity current. A sample calculation using experimental data is included in Appendix A.

The calculations show that, using reasonable values for the above parameters, overriding turbidity currents in a full-scale fluviodeltaic system can reduce foreset slopes to 2-5°. By extension, this suggests that if a system strongly influenced by turbidity currents encounters relatively subdued basement slopes, sediment deposition on the foreset may be impeded and it may become un-choked. Interestingly, these slopes are comparable to slopes we observe on modern continental margins (Pratson & Haxby, 1996).

VI. DISCUSSION

The conceptual model and experiments illustrate that sediment flux across the forset toe in a linked fluviodeltaic system exerts an important influence on the overall evolution of the system and resulting stratigraphy. The foreset toe functions as a critical point in the clinoform system. The experiments show that the toe sediment flux can be controlled by mechanisms other than changes in sea level or bedload sediment supply. Further, the experiments demonstrate that when the sediment flux across the delta toe is changed, the impact propagates through the entire fluvial system, suggesting that fluvial behavior, even in upstream reaches, can be strongly controlled by offshore sediment dynamics. These findings are in profound contrast to the sequence-stratigraphic model, where fluvial sedimentation is controlled principally by changes in sea level.

A. STRATIGRAPHIC IMPLICATIONS

The basic sequence-stratigraphic model predicts deposition of coarse-grained "basin-floor fans" during sea-level lowstands as a result of fluvial incision and sediment bypass. The sequence stratigraphic argument for sand transfer to the deep marine system during lowstand is fundamentally based on the "A/S ratio concept" (Jervey, 1988). During lowstand, deposition occurs seaward of the shoreline because this is the only place in the linked fluviodeltaic system where accommodation exceeds sediment supply (i.e. $A/S > 1$).

The results of this study, when viewed in the context of the A/S ratio concept, contradict the predictions of the sequence stratigraphic model. In the conceptual and experimental scenarios presented above, there is no change in relative sea level and based

on the traditional definition, the rate of creation of accommodation is zero (A = 0). With the "ramp" geometry, there is a gradual increase in accommodation as the delta progrades further basinward, but $A \rightarrow 0$ once the delta has reached the base of the ramp. The sediment supply in the conceptual model and experiments is always greater than zero and always exceeds the rate of creation of accommodation space (i.e. $A/S < 1$). Under these conditions, the sequence stratigraphic model would prediction a progradational shoreline for all time. Only if the rate of sea level rise increased so that it exceeded sediment supply would the shoreline become retrogradational. In my conceptual model and experiments, however, shoreline progradation was arrested, despite the fact that sediment supply continued to exceed accommodation ($A/S < 1$).

The sequence-stratigraphic model predicts fluvial incision and deposition of coarse-grained fluvial sediment in deeper portions of the basin during periods of sea level fall and lowstand. Fundamentally, this is because during sea level fall and lowstand, the rate of accommodation space creation becomes small, while sediment supply remains fixed (A/S becomes $<< 1$). This results in "forced regression" of the shoreline, fluvial incision, and sand transfer to the deep marine portions of the basin. My conceptual model and supporting experiments suggest an alternative mechanism for sand transfer to the deep marine. Using the choke point concept presented here, sand transfer to the deep marine occurs because, for any of a number of reasons, sediment cannot accumulate at the foreset toe, which in turn prevents sedimentation on the foreset and deposition in the fluvial system. Note, however, that the A/S ratio remains constant during the period of offshore deposition.

The recent work of Brown et al. (2004) provides a nice example of the potential implications of these competing models. Based on extensive seismic and well-log data, Brown et al. (2004) present a detailed model for the filling of intraslope subbasins in the Gulf of Mexico. The model predicts delta progradation to near the shelf edge during relative-sea-level highstands. As the delta interacts with the shelf edge, muddy sediments are deposited on the lower slope due to failure and slumping of the delta front; sand-rich sediment is stored in the fluvial system and not transferred to the deeper basin (Figure 15A). With the delta at the shelf edge, the Brown et al. (2004) model invokes a sea-level fall that causes fluvial incision and bypass, cessation of delta progradation, and routing of coarse sediment to the deeper basin, resulting in deposition of basin-floor and slope fans (Figure 15B). Sediment loading of the basin floor drives rotation on a major syndepositional growth-fault system; this rotation forms an intraslope subbasin bounded seaward by a shale ridge. Brown et al. (2004) then call upon a rise in relative sea level to rejuvenate delta progradation across the previously deposited (and subsequently rotated) basin-floor and slope fans (Figure 15C). Progradation and filling of the subbasin continues until the delta toe interacts with the basinward shale ridge, which forms the effective shelf edge, at which time the cycle of fluvial bypass and deposition of basin-floor fans begins anew.

While the Brown et al. (2004) model provides a possible explanation for the stratigraphic patterns observed in intraslope subbasins, it relies on coincidental events. First, the maximum rate of sea level fall that leads to fluvial incision must occur precisely when the delta toe has reached the shelf edge. While this is possible, it seems unlikely

that the periodicity of sea level change would coincide exactly with the time required for the delta to reach the shelf edge. Furthermore, it seems doubtful that same events would occur repeatedly in order to form the series of sequences observed by Brown et al (2004).

My conceptual model and supporting experimental results provide a potentially simpler explanation for the formation of sequences similar to those observed by Brown et al. (2004) that does not require a change in sea level (compare Figure 15D and Figure 13C). The failure and slumping of delta-front sediments that occurs when the delta reaches the steep shelf edge minimizes sediment deposition on the foreset and "un-chokes" the clinoform system. With no deposition occurring on the foreset, deposition in the fluvial system ceases. Coarse-grained sediment bypasses the fluvial system and is routed to the deeper basin, forming basin-floor fans that eventually onlap the slope. Once the fluvial sediments have filled the subbasin, the delta is again able to prograde until it reaches the steep topography at the next shale ridge. Thus, we suggest that the basin-floor fans in these stratigraphic sequences may have been formed by "un-choking" the clinoform system and are not necessarily due to a change in sea level. In this case, sand is transferred to the deep marine basin simply because the delta encounters a bathymetric slope steeper than the foreset slope and deposition on the foreset is impeded. This change in dynamics on the foreset is translated up-dip, ultimately resulting in fluvial bypass and sand transfer to the basin floor. Sustained turbidity currents passing over the delta foreset during progradation would act to the lower the stable foreset slope and make "un-choking" the system possible with even lower bathymetric slopes.

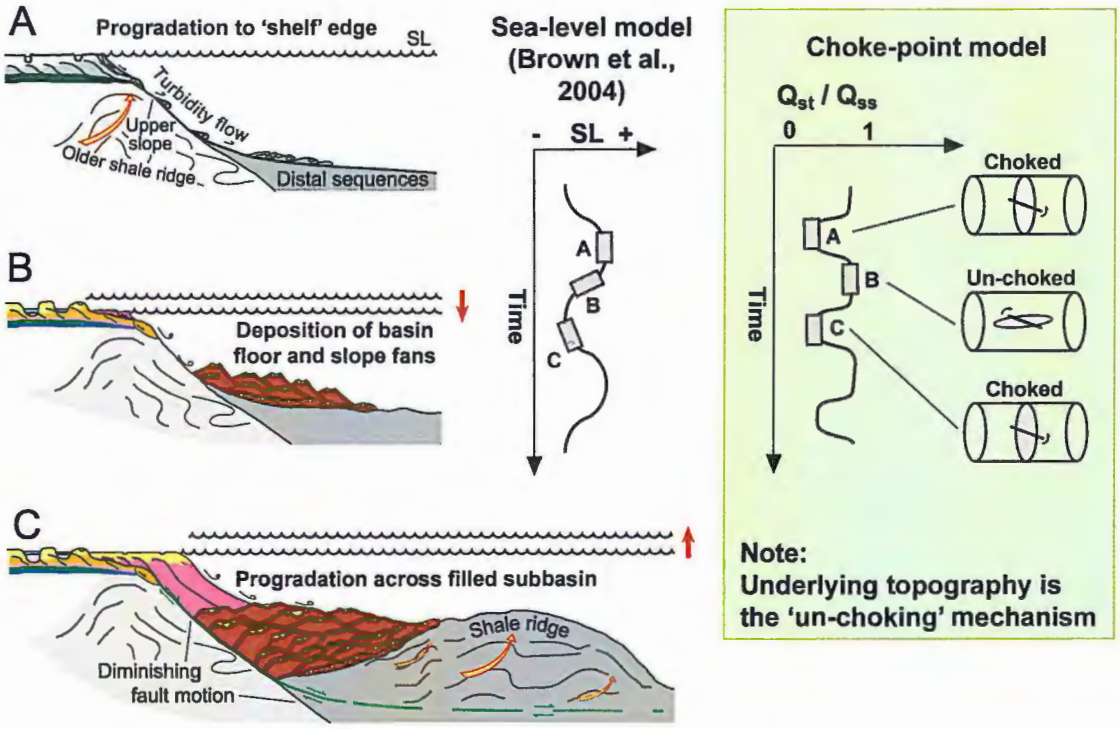

Figure 15. Model for filling growth-faulted, intraslope subbasins (Brown et al., 2004) (A) Delta reaches the edge of the slope and distal deposition of mud begins via turbidity currents. (B) With delta at the shelf edge, sea level begins to fall. During maximum rate of sea level fall, fluvial incision occurs, accompanied by deposition of basin-floor fans. (C) Sea level begins to rise and delta progrades across filled subbasin. Cycle is repeated when delta reaches the edge of the next shale ridge.

A second stratigraphic implication of my experiments concerns fluvial incision. An increase in sediment supply to the fluvial system is generally thought to cause fluvial aggradation (Lane, 1955). My experiments show that an increase in *suspended* sediment supply to the system can cause readjustment of the delta foreset angle, changing fluvial dynamics and resulting in autogenic knickpoint generation and fluvial incision. In addition, a commonly invoked mechanism for generating widespread fluvial incision is relative sea level fall (Posamentier & Vail, 1988; Van Wagoner et al., 1990). My results show that erosion of the fluvial system can readily be produced without changing sea

level. Thus fluvial incision caused by our proposed mechanism could be misinterpreted as due to a fall in relative sea level, especially at the outcrop scale. However, it is unlikely that my model could generate widespread and significant incision seen at the seismic scale (a true "Type I" sequence boundary in the sequence stratigraphic model). The stratigraphic implications of my model would be more likely observed at the outcrop scale, where sequence boundary identification can be much more difficult due to the complex interplay of allogenic and autogenic processes that cannot be seen in large-scale seismic studies.

Results from my experiments may explain partly the fluvial incision observed in the Brown et al. (2004) sequences. As shown in Figures 13C and 13D, fluvial incision occurred in the experiments as a result of turbidity current activity that caused a reduction in the foreset slope. Brown et al. (2004) predict turbidity current activity during Stage 1 of their model. Slight variation in the turbidity current concentration could cause temporary reductions of the delta foreset slope, which would in turn drive fluvial incision as observed in my experiments.

While the choke point mechanism would result in some fluvial incision, it is unlikely that it would be of a comparable scale (~100 m) to that observed by Brown et al (2004). A possible explanation for this could be continued rotation of the shale ridge as sediment loading continues. This "upflift" might be sufficient to generate a fall in relative sea level, which could act to increase the amount of fluvial incision that would occur when the delta was un-choked.

B. CONCLUSIONS

My key finding is that preventing sediment from accumulating at the delta toe freezes the fluviodeltaic system and facilitates transfer of sand to the deep-marine portion of the system. This is true regardless of the mechanism used to inhibit sedimentation at the toe – for example, though I have not tested it, waves might produce similar effects in combination with steep basement slopes. Fluvial bypass and sand transfer have significant stratigraphic implications. Typically, the mechanism invoked to deliver sand to the deep-water basin is a sea level fall below the shelf edge (Van Wagoner et al., 1990). But the work we report here shows that sand can be efficiently transported to deep water with no change in sea level. Morphologically, the sandy deposits resemble "low-stand fans," composed of material eroded from the shelf edge during a sea level fall.

From a sequence-stratigraphic perspective, perhaps the most significant result of my model is that features generally associated with the LST (low-stand fans, fluvial incision) can be formed during the HST. My model provides an alternative explanation for the formation of stratigraphic features often interpreted to result from a change in relative sea level. Given these results, care should be exercised when using the sequence stratigraphic model to make stratigraphic correlations and reconstruct relative sea level. My model shows that the sediment flux in different parts of a fluviodeltaic system can be controlled by mechanisms other than relative sea level and that changes in sea level are not a unique mechanism for the creation of many stratigraphic features.

APPENDIX A: SAMPLE CALCULATION – FROUDE NUMBER SCALING

The first step in scaling the turbidity current experiments is to calculate the shear stress due to overpassing turbidity current in the experiment, i.e. find $(\tau_t^*)_m$ using Equation (A-1).

$$\tan\theta_a = \tan\theta_{ao}\left(1 - \frac{1}{\cos\theta_a}\frac{\tau_t^*}{\tau_{co}^*}\right) \tag{A-1}$$

Rearranging, we have

$$\tau_t^* = \left(\frac{\tan\theta_a}{\tan\theta_{ao}} - 1\right)\left(-\cos\theta_a \cdot \tau_{co}^*\right) \tag{A-2}$$

For experiment X, $\theta_a = 25.0°$ and $\theta_{ao} = 30.4°$

The critical Shield stress τ_{co}^* is typically found to be in the range 0.03-0.04 (Graf, 1971).

For this example, we take $\tau_{co}^* = 0.04$. Then, plugging these values into Equation (A-2), we obtain

$$\tau_t^* = \left(\frac{\tan\theta_a}{\tan\theta_{ao}} - 1\right)\left(-\cos\theta_a \cdot \tau_{co}^*\right) = \left(\frac{\tan(25.0°)}{\tan(30.4°)} - 1\right)\left(-\cos(25.0°)\cdot 0.04\right) = 0.00743 \tag{A-3}$$

To scale this Shield stress to field scale, we use the following relation obtained from the requirement that the densimetric Froude number in the experiment is equal to that in the full-scale system (see main text for details).

$$\frac{(\tau_t^*)_p}{(\tau_t^*)_m} = (\lambda_H)^{5/6}(\lambda_C)(\lambda_D)^{-1} \tag{A-4}$$

Rearranging, we have

$$(\tau_t^*)_p = (\tau_t^*)_m(\lambda_H)^{5/6}(\lambda_C)(\lambda_D)^{-1} \tag{A-5}$$

For the sample calculation, we choose the following: $\lambda_H = 100$, $\lambda_C = 0.1$, and $\lambda_D = 1$.

Plugging in these values, we obtain

$$(\tau_t^*)_p = (\tau_t^*)_m (\lambda_H)^{5/6} (\lambda_C)(\lambda_D) = (0.00743) \cdot (100)^{5/6} \cdot (0.1) \cdot (1) = 0.0345 \qquad \text{(A-6)}$$

Now, we can calculate the foreset angle for this shear stress by iteratively solving Equation (A-1) for θ_a. The solution for various values of τ_{co}^* is presented graphically in Figure A-1.

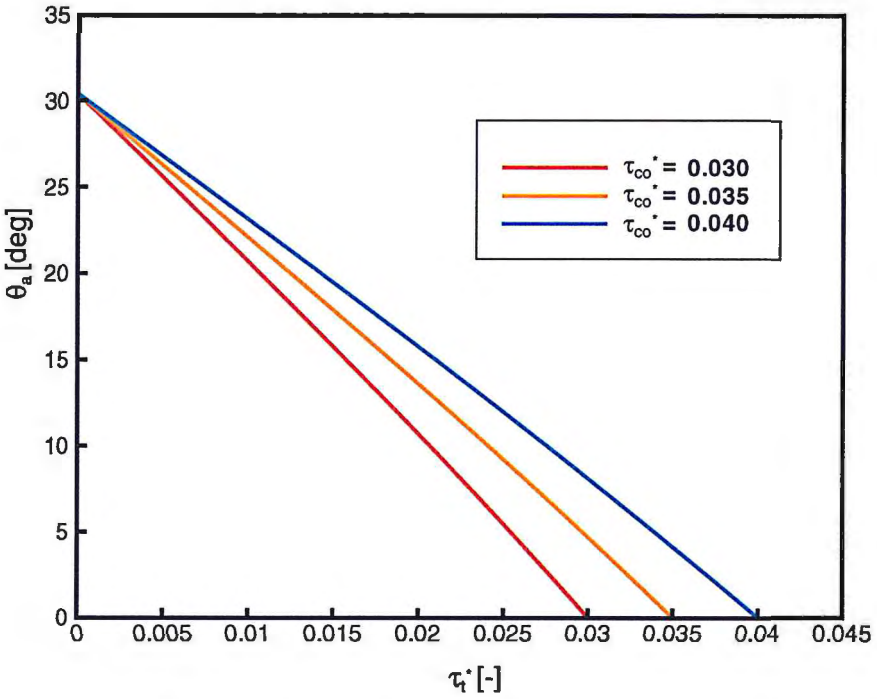

Figure A-1. Solution to Equation A-1 for various values of τ_{co}^*.

Referring to Figure A-1, we see that for $\tau_t^* = 0.0345$, $\theta_a \sim 4.5°$. Thus, the 18% decrease in foreset slope observed in the experiment corresponds to an 85% decrease in foreset slope at a field scale. Furthermore, this calculation shows that, using reasonable scaling approximations, turbidity currents can lower delta foreset slopes to gradients commonly observed in geologic settings. This suggests that the un-choking phenomenon may not be limited to geologic settings with high slopes (e.g. tectonically active areas), but may occur in settings with more typical subdued slopes.

BIBLIOGRAPHY

Allen, P.A., and Allen, J.R., 1990, Basin Analysis: Principles and Applications, Blackwell Science, Oxford, 451 p.

Blum, M.D., and Törnqvist, T.E., 2000, Fluvial responses to climate and sea-level change: a review and look forward, *Sedimentology* 47 (Suppl. 1), 2-48.

Brown, L.F., Loucks, R.G., Trevino, R.H., and Hammes, U., Understanding growth-faulted, intraslope subbasins by applying sequence-stratigraphic principles: examples from the south Texas Oligocene Frio Formation, *AAPG Bulliten* 88, 1501-1522.

Fisk, H.N., 1944, Geological Investigations of the Alluvial Valley of the Lower Mississippi River, Mississippi River Commission, Vicksburg.

Gilbert, G.K., 1877, Report on the Geology of the Henry Mountains, Government Printing Office, Washington, DC.

Gilbert, G.K., 1890, Lake Bonneville, U.S. Geological Survey Monograph 1, Government Printing Office, Washington, D.C.

Graf, W.H., 1971, Hydraulics of Sediment Transport, McGraw-Hill, New York, 513 p.

Haq, B.U., Hardenbol, J., and Vail, P.R., 1987, Chronology of fluctuating sea levels since the Triassic, *Science* 235, 1,156-1,166.

Helland-Hansen, W., and Gjelberg, J.G., 1994, Conceptual basis and variability in sequence stratigraphy: a different perspective, *Sedimentary Geology* 92, 31-52.

Jervey, M.T., 1988, Quantitative geological modeling of siliciclastic rock sequences and their seismic expression, *in* Wilgus, C.K., Hastings, B.S., Kendall, C.G. St. C., Posamentier, H.W., Ross, C.A., and Van Wagoner, J.C., eds., Sea Level Changes—An Integrated Approach, SEPM Special Publication 42, 125-154.

Kostic, S., Parker, G., and Marr, J.G., 2002, Role of turbidity currents in setting the foreset slope of clinoforms prograding into standing fresh water, *Journal of Sedimentary Research* 72, 353–362.

Lane, E.W., 1955, The Importance of Fluvial Morphology in Hydraulic Engineering, *American Society of Civil Engineers, Proceedings* 81, 1-17.

Mackin, J.H., 1948, Concept of the graded river, *Geological Society of America Bulletin* 59, 463-512.

Milligan, M.R., and Chan, M.A., 1998, Coarse-grained Gilbert deltas: facies, sequence stratigraphy and relationships to Pleistocene climate at the eastern margin of Lake Bonneville, northern Utah, *in* Shanley, K.W., and McCabe, P.J., eds., Relative Role of Eustasy, Climate, and Tectonism in Continental Rocks, SEPM Special Publication 59, 177-190.

Muto, T., and Steel, R.J., 1997, Principles of regression and transgression: the nature of the interplay between accommodation and sediment supply, *Journal of Sedimentary Research* 67, 994-1000.

Muto, T., and Steel, R.J., 2000, The accommodation concept in sequence stratigraphy: some dimensional problems and possible redefinition, *Sedimentary Geology* 130, 1-10.

Muto, T., and Steel, R.J., 2002, Role of autoretreat and A/S changes in the understanding of deltaic shoreline trajectory: a semi-quantitative approach, *Basin Research* 14, 303-318.

Paola, C., 2000, Quantitative models of sedimentary basin filling, *Sedimentology* 47 (Suppl. 1), 121-178.

Paola, C., Mullin, J., Ellis, C., Mohrig, D.C., Swenson, J.B., Parker, G., Hickson, T., Heller, P.L., Pratson, L., Syvitski, J., Sheets, B., and Strong, N., 2001, Experimental Stratigraphy, *GSA Today*, July 2001, 4-9.

Pirmez, C., Pratson, L.F., and Steckler, M.S., 1998, Clinoform development by advection-diffusion of suspended sediment: Modeling and comparison to natural systems, *Journal of Geophysical Research* 103, 24,141-24,157.

Porębski, S.J., and Steel, R.J., 2003, Shelf-margin deltas: their stratigraphic significance and relation to deepwater sands, *Earth-Science Reviews* 62, 283-326.

Posamentier, H.W., and Allen, G.P., 1999, Siliclastic sequence stratigraphy – Concepts and applications, SEPM Concepts in Sedimentology and Paleontology 7, 210 pp.

Posamentier, H.W., and James, D.P., 1993, Sequence stratigraphy—uses and abuses, *in* Posamentier, H.W., Summerhayes, C.P., Haq, B.U., and Allen, G.P., eds., Sea Level Changes—An Integrated Approach, SEPM Special Publication 42, 3-18.

Posamentier, H.W., and Vail, P.R., 1988, Eustatic controls on clastic deposition II – sequence and systems tract models, *in* Wilgus, C.K., Hastings, B.S., Kendall,

C.G. St. C., Posamentier, H.W., Ross, C.A., and Van Wagoner, J.C., eds., Sea Level Changes—An Integrated Approach, SEPM Special Publication 42, 125-154.

Powell, J.W., 1875, Exploration of the Colorado River of the West, Washington, D.C., U.S. Government Printing Office, 291 p.

Pratson, L.F., and Haxby, W.F., 1996, What is the slope of the U.S. continental slope?, *Geology* 24, 3-6.

Rich, J.L., 1951, Three critical environments of deposition, and criteria for recognition of rocks deposited in each of them, *Geological Society of America Bulletin* 62, 1-19.

Saucier, R.T., 1981, Current thinking on riverine processes and geologic history as related to human settlement in the southeast, *Geoscience and Man* 22, 7-18.

Sangree, J.B., and Windmier, J.M., 1977, Seismic stratigraphy and global changes in sea level, part 9: Seismic interpretation of depositional facies, *in* C.W. Payton, ed., Seismic stratigraphy—Applications to hydrocarbon exploration: AAPG Memoir 26, 165-184.

Schumm, S.A., 1993, River Response to Baselevel Change: Implications for Sequence Stratigraphy, *Journal of Geology* 101, 279-294.

Sloss, L.L., 1962, Stratigraphic models in exploration, *Journal of Sedimentary Petrology* 32, 415-422.

Steel, R.J., and Olsen, T., 2002, Clinoforms, Clinoform Trajectories and Deepwater Sands, *in* Proceedings, 22nd Annual Gulf Coast Section SEPM Foundation Bob F. Perkins Research Conference.

Swenson, J.B., Paola, C., Pratson, L., Voller, V.R., and Murray, A.B., 2005, Fluvial and marine controls on combined subaerial and subaqueous delta progradation: Morphodynamic modeling of compound-clinoform development, *Journal of Geophysical Research* 110, F02013, doi:10.1029/2004JF000265.

Swenson, J.B., Voller, V.R., Paola, C., Parker, G., and Marr, J.G., 2000, Fluvio-deltaic sedimentation: A generalized Stefan problem, *European Journal of Applied Mathematics* 11, 433-452.

Swift, D.J.P., Hudelson, P.M., Brenner, R.L., and Thompson, P., 1987, Shelf construction in a foreland basin: storm beds, shelf sandbodies, and shelf-slope depositional

sequences in the Upper Cretaceous Mesaverde Group, Book Cliffs, Utah, *Sedimentology* 34, 423-457.

Vail, P.R., Mitchum, R.M., and Thompson III, S., 1977, Seismic stratigraphy and global changes in sea level, part 3: Relative changes in sea level from coastal onlap, *in* C.W. Payton, ed., Seismic stratigraphy—Applications to hydrocarbon exploration: AAPG Memoir 26, 63-97.

Van Wagoner, J.C., Mitchum, R.M., Campion, K.M., and Rahmanian, V.D., 1990, Siliciclastic Sequence Stratigraphy in Well Logs, Cores, and Outcrops, AAPG Methods in Exploration 7, 55 p.

Walsh, J.P., and Nittrouer, C.A., 2003, Contrasting stlyles of off-shelf sediment accumulation in New Guinea, *Marine Geology* 196, 105-125.